Carbohydrate Polymers 82 (2010) 585–593

Contents lists available at ScienceDirect

Carbohydrate Polymers

journal homepage: www.elsevier.com/locate/carbpol

Effect of lipid self-association on the microstructure and physical properties of hydroxypropyl-methylcellulose edible films containing fatty acids

A. Jiménez, M.J. Fabra, P. Talens*, A. Chiralt

Departamento Tecnología de Alimentos-Instituto Universitario de Ingeniería de Alimentos para el Desarrollo, Universidad Politécnica de Valencia, Camino de Vera, s/n 46022, Valencia, Spain

ARTICLE INFO

Article history:
Received 9 April 2010
Received in revised form 7 May 2010
Accepted 11 May 2010
Available online 21 May 2010

Keywords:
Emulsified films
Lipid particle size
Water vapour permeability
Tensile properties
Scanning electron microscopy

ABSTRACT

The effect of saturated and unsaturated fatty acids on hydroxypropyl-methylcellulose (HPMC) based films was studied. Edible films based on HPMC containing lauric (LA), miristic (MA), palmitic (PA), stearic (SA) and oleic (OA) acids were obtained with 1:0.15 polymer–lipid ratio. The particle size distribution and rheological behaviour of the film-forming emulsions were studied, as well as the cross-section and surface microstructure of dried films. The effect of the film microstructure on its mechanical, optical and water barrier properties was analyzed. Saturated LA, MA and PA formed bigger lipid micellar structures than SA and OA in the HPMC aqueous system, which grew notably during film drying, giving rise to crystallized lipid layers in the films which were not observed for SA and OA. Laminar structures improved the moisture barrier properties, but resulted in more brittle, less stretchable, more opaque and less glossy films, depending on the particle size.

1. Introduction

An edible film or coating is defined such as a thin film formed by edible compounds which act as a barrier against external compounds (moisture, oxygen, gases, aromas) so that protects the product and increases its shelf-life (Guilbert, Gontard, & Gorris, 1996). Furthermore, the use of edible films in food packaging would reduce the amount of domestic waste thus contributing to minimize the environmental pollution.

These films are generally made with lipids and/or hydrocolloid such as edible fats, fatty acids, proteins and polysaccharides. A large number of works has been published using proteins in the formulation of edibles films (Albert & Mittal, 2002; Gómez-Estaca, Giménez, Montero, & Gómez-Guillén, 2009; Mecitoğlu, Yemenicioğlu, & Arslanoğlu, 2007; Monedero, Fabra, Talens, & Chiralt, 2009; Pérez-Gago & Krochta, 2001) and polysaccharides (Albert & Mittal, 2002; Mathew & Abraham, 2008; Sánchez-González, Vargas, González-Martínez, Chiralt, & Cháfer, 2009; Villalobos, Hernández-Muñoz, & Chiralt, 2006).

Polysaccharide based films show good mechanical properties and act as an effective barrier against gases, thus contributing to increase the shelf-life of foods without creating anaerobic conditions (Baldwin, Nisperos-Carriedo, & Baker, 1995a, 1995b). However, as a consequence of their hydrophilic nature, polysaccharide based films constitute poor moisture barriers (Turhan & Şahbaz, 2004).

Several cellulose derivated materials such as methylcellulose, carboxymethylcellulose, and hydroxypropyl-methylcellulose have been used in the preparation of edible films (Albert & Mittal, 2002; Sánchez-González et al., 2009; Villalobos et al., 2006). HPMC presents excellent film-forming properties but the reduction of its hydrophilic character is necessary to improve its functionality. Waxes have been studied as hydrophobic compounds to improve the water barrier properties of edible films (Pérez-Gago & Krochta, 2001). Actually these are being questioned due to its effect on human health by many organizations. During last two decades different works studied the use of fatty acids as lipid components to be incorporated in hydrophilic films to modulate the water vapour barrier properties of protein (Fabra, Jiménez, Atarés, Talens, & Chiralt, 2009; Fernández, Díaz de Apodaca, Cebrián, Villarán, & Maté, 2007) and polysaccharide based films (Hagenmaier & Shaw, 1990; Koelsch & Labuza, 1992).

Fatty acids are characterized by their chain length and unsaturation degree and both have an important influence on their technological applications (Fernández et al., 2007). This provides to fatty acids different properties such as variable reactivity and different physical state at room temperature. Another particular characteristic of these polar lipids is their tendency to self-association in aqueous systems giving rise to different micellar structures, depending on the affinity with their aqueous environment and the hydrophobic forces (Krog, 1990). These molecular aggregations in the aqueous film-forming dispersions can develop

* Corresponding author. Tel.: +34 963879836; fax: +34 963877369.
E-mail address: pautalens@tal.upv.es (P. Talens).

0144-8617/$ – see front matter © 2010 Elsevier Ltd. All rights reserved.
doi:10.1016/j.carbpol.2010.05.014

during the films drying since they show lyotropic mesomorphism and micellar phase transition can occur in line with the reduction of the solvent availability. In dry films, polar lipid can crystallize or not in separated laminar associations of different size depending on the molecular interactions in the aqueous media. A recent work studied the final microstructure of sodium caseinate films containing fatty acids, showing the relevant role that the formations of big layers of crystallized lipid in the dried films play in the water barrier properties. In this sense, lauric acid which formed the biggest lipid layers, perpendicular to the mass transfer direction showed the minimum value of water vapour permeability (Fabra et al., 2009).

On the other hand, interactions of fatty acids with hydrocolloid, especially proteins (Erickson, 1990; Fabra, Talens, & Chiralt, 2010) and starch (Mondragón, Arroyo, & Romero-García, 2008) have been widely described. These interactions can affect not only the lipid self-association process in the FFD, but the crosslinking process responsible for the formation of the film network and so the functional film properties.

In this work, the influence of fatty acids of different chain length or instauration level on the microstructural properties of film-forming dispersions and films of hydroxylpropyl-methylcellulose was analyzed, as well as their impact on the relevant properties of the film that ensure its suitability as food coating: water vapour barrier, mechanical and optical properties.

2. Materials and methods

2.1. Materials

Hydroxypropyl-methylcellulose (HPMC) was obtained from Fluka (Sigma–Aldrich Chemie, Steinheim, Germany). Fatty acids (minimum purity 96%) were purchased from Panreac Quimica, S.A. (Castellar Del Vallés, Barcelona, Spain). The fatty acids used were lauric (LA, $C_{12:0}$), miristic (MA, $C_{14:0}$), palmitic (PA, $C_{16:0}$), stearic (SA, $C_{18:0}$) and oleic (OA, $C_{18:1}$).

2.2. Preparation and characterization of film-forming dispersions

The film-forming aqueous dispersions (pH = 7.4) of the control film (HPMC) contained 4% (w/w) HPMC. The protein:lipid ratio in emulsified films was 1:0.15. Except in the case of OA (which is liquid at room temperature) lipid was added to the previously heated (85 °C) HPMC dispersions to favour the lipid dispersion in the system. The emulsions were homogenized at 13,500 rpm for 1 min and at 20,500 rpm for 3 min using a rotor-stator homogenizer (Ultraturrax T25, Janke and Kunkel, Germany). Finally, they were chilled to room temperature during 2 h and degasified at 7 mbar with a vacuum pump (Wertheim, Germany). Dispersion of OA was prepared without heating, at room temperature to avoid oxidation phenomena.

2.2.1. Lipid particle size

The droplet size distribution, weight mean diameter ($D_{4,3}$) and volume-surface mean diameter ($D_{3,2}$) were determined in triplicate with a laser light scattering instrument (Malvern Mastersizer, Malvern Instruments, Worcestershire, U.K.). Lipid particle size measurements were done on the film-forming emulsion. $D_{4,3}$ is the average size based on the unit weight of particles, whereas $D_{3,2}$ represents the average size based on the specific surface per unit volume. These parameters are described by Eqs. (1) and (2), where n_i is the number of droplets of a determined size range and d_i is the droplet diameter:

$$D_{4,3} = \frac{\sum n_i d_i^4}{\sum n_i d_i^3} \quad (1)$$

$$D_{3,2} = \frac{\sum n_i x d_i^3}{\sum n_i d_i^2} \quad (2)$$

2.2.2. Rheological behaviour

The rheological behaviour of the film-forming emulsions was analyzed in triplicate at 25 °C by means of a rheometer (HAAKE Rheostress 1, Thermo Electric Corporation, Karlsruhe, Germany) with a coaxial cylinders sensor (Z34DIN Ti). Rheological curves were obtained after resting the sample in the sensor for 5 min at 25 °C. The shear stress (σ) was measured as a function of shear rate ($\dot{\gamma}$) from 0 to 512 s^{-1}. The Newton model was applied to determine the viscosity of the emulsions.

2.3. Preparation and characterization of films

Each film was prepared by weighing the amount of film-forming emulsion containing 2 g of total solids. This mass of emulsion was spread evenly over a Teflon casting plate (15 cm diameter) resting on a level surface, and films were formed by drying for approximately 48 h at 45% RH and 20 °C. Dry films could be peeled intact from the casting surface. Film thickness was measured with a Palmer digital micrometer to the nearest 0.0025 mm at 4–6 random position depending of the analysis.

2.3.1. Tensile properties

A universal test Machine (TA.XTplus model, Stable Micro Systems, Haslemere, England) was used to determine the tensile strength (TS), elastic modulus (EM), and elongation (E) of the films, according to ASTM standard method D882 (ASTM, 2001) EM, TS, and E were determined from the stress–strain curves, estimated from force-distance data obtained for the different films (2.5 cm wide and 10 cm long). Right six replicates were analyzed per formulation. Before testing, samples were equilibrated for one week at 10 °C and at 58% RH using magnesium nitrate-6-hydrate saturated solutions (Panreac Quimica, SA, Castellar del Vallés, Barcelona). Equilibrated specimens were mounted in the film-extension grips of the testing machine and stretched at 50 mm min^{-1} until breaking. The relative humidity of the environment was held constant at 58 (±2)% during the tests, which were performed at 10 (±1) °C.

2.3.2. Water vapour permeability

A modification of the ASTM E96-95 gravimetric method (Mc Hugh, Avena-Bustillos, & Krochta, 1993) for measuring WVP of flexible films was employed for all films using Payne permeability cups (3.5 cm diameter, Elcometer SPRL, Hermelle/s Argenteau, Belgium). Films were selected for WVP tests based on lack of physical defects such as cracks, bubbles, or pinholes. Distilled water was placed in each cup to expose the film to 100% RH on one side. Once the films were secured, each cup was placed in a relative humidity equilibrated cabinet fitted with a fan to provide a strong driving force across the film for water vapour diffusion. RH of the cabinets (58% at 10 °C or 54% at 20 °C) was held constant using oversaturated solutions of magnesium nitrate-6-hydrate (Panreac Quimica, SA, Castellar del Vallés, Barcelona). The free film surface during film formation was always exposed to lowest relative humidity. The cabinets were placed at a controlled temperature of 10 or 20 °C. The cups were weighed periodically (0.0001 g). Water vapour transmission (WVTR) was determined from the slope obtained from the regression analysis of weight loss data versus time, once the steady state had been reached, divided by the film area.

From WVTR data, the vapour pressure on the film's inner surface (p_2) was obtained with Eq. (3), proposed by Mc Hugh et al. (1993) to correct the effect of concentration gradients established in the

stagnant air gap inside the cup:

$$\mathrm{WVTR} = \frac{P \cdot D \cdot \mathrm{Ln}[(P - p_2)/P - p_1]}{R \cdot T \cdot \Delta z} \quad (3)$$

where P, total pressure (atm); D, diffusivity of water through air at 10 and 20 °C (m^2/s); R, gas law constant ($82.057 \times 10^{-3}\ m^3\ atm\ kmol^{-1}\ K^{-1}$); T, absolute temperature (K); Δz, mean stagnant air gap height (m), considering the initial and final z value; p_1, water vapour pressure on the solution surface (atm); and p_2, corrected water vapour pressure on the film's inner surface (atm). Water vapour permeance was calculated using Eq. (4) as a function of p_2 and p_3 (pressure on the film's outer surface in the cabinet).

$$\mathrm{permeance} = \frac{\mathrm{WVTR}}{p_2 - p_3} \quad (4)$$

Permeability was obtained by multiplying the permeance by the average film thickness.

2.3.3. Scanning electron microscopy (SEM)

Microstructural analysis of the films was carried out using a scanning electron microscope (JEOL JSM-5410, Japan). Film samples were maintained in a desiccator with P_2O_5 for two weeks. Then films were frozen in liquid N_2 and gently and randomly broken to investigate the cross-section of the samples. Films were fixed on copper stubs, gold coated, and observed using an accelerating voltage of 10 kV.

2.3.4. Atomic force microscopy (AFM)

Water of film samples was previously eliminated by using a desiccator with P_2O_5. The surface morphology of the films was analyzed by using AFM with a Nanoscope III.a, Scanning Probe Microscope (Digital Instruments, Inc., Santa Barbara, CA) with a 125 μm × 125 μm scan size and a 6 μm vertical range. The resulting data set of each sample was transformed into a 3D image and into a grey scale mode map. Measurements were taken from several areas of film surface (50 μm × 50 μm) using the tapping mode. According to the method ASME B46.1 (ASME, 1995) the following statistical parameters related with sample roughness were calculated: average roughness (R_a: average of the absolute value of the height deviations from a mean surface), root-mean-square roughness (R_q: root-mean-square average of height deviations taken from the mean data plane), and factor of roughness (r: ratio between the three-dimensional surface and two-dimensional area projected onto the threshold plane). Three images were analyzed in each case.

2.3.5. Optical properties

The transparency was determined by applying the Kubelka–Munk theory (Hutchings, 1999) for multiple scattering to the reflection spectra. As the light passes through the film, it is partially absorbed and scattered, which is quantified by the absorption (K) and the scattering (S) coefficients. Internal transmittance (T_i) of the films was quantified using Eq. (5). In this equation R_0 is the reflectance of the film on an ideal black background. a and b parameters are calculated by Eqs. (6) and (7) where R is the reflectance of the sample layer backed by a known reflectance R_g. The surface reflectance spectra of the films were determined from 400 to 700 nm with a spectrocolorimeter CM-3600d (Minolta Co., Tokyo, Japan) on both a white and a black background. L^*, a^* and b^* values from the CIELAB colour space were determined using D65 illuminant and 10° observer and taking into account R_∞ (Eq. (8)) which correspond with the reflectance of an infinitely thick layer of the material. From these values whiteness index (WI) were obtained (Eq. (9)). Measurements were taken in triplicate for each sample considering the free film surface during film formation:

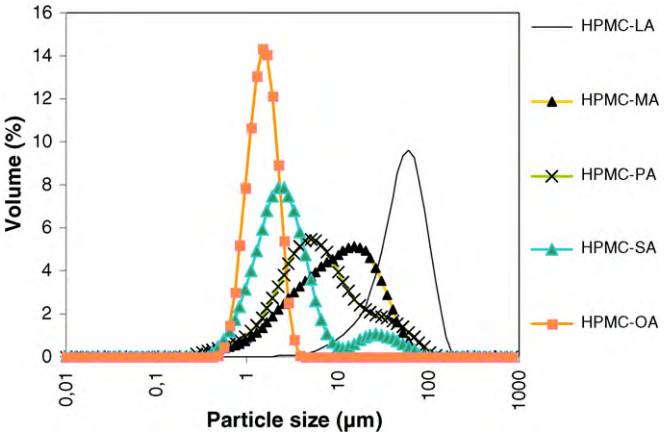

Fig. 1. Particle size distribution of film-forming emulsions.

$$T_i = \sqrt{(a - R_0)^2 - b^2} \quad (5)$$

$$a = \frac{1}{2} \cdot \left(R + \frac{R_0 - R + R_g}{R_0 R_g} \right) \quad (6)$$

$$b = (a^2 - 1)^{1/2} \quad (7)$$

$$R_\infty = a - b \quad (8)$$

$$\mathrm{WI} = 100 - \sqrt{(100 - L^*)^2 + a^{*2} + b^{*2}} \quad (9)$$

The gloss was measured on the free film surface during film formation, at 20° and 60° angles from the normal to the surface, according to the ASTM standard D523 method (ASTM, 1999) using a flat surface gloss meter (Multi.Gloss 268, Minolta, Germany). Measurements were taken in triplicate for each sample and three films of each formulation were considered. All results are expressed as gloss units, relative to a highly polished surface of black glass standard with a value near to 100.

2.4. Statistical analysis

Statistical analyses of data were performed through analysis of variance (ANOVA) using Statgraphics Plus for Windows 5.1 (Manugistics Corp., Rockville, MD). Fisher's least significant difference (LSD) procedure was used at the 95% confidence level.

3. Results and discussion

3.1. Characterization of the film-forming emulsions

3.1.1. Lipid particle size

The study of the lipid particle size, as well as their distribution in the film-forming emulsions, is of interest because of its impact on the film microstructure and physical properties, such as water vapour permeability, mechanical properties, and general barrier properties (Bravin, Peressini, & Sensidoni, 2004; Pérez-Gago & Krochta, 2001). Fig. 1 shows the particle size distribution for the film-forming emulsions and values of mean diameters $D_{3,2}$ and $D_{4,3}$ are shown in Table 1. All the distributions were monomodal, as previously reported by Sánchez-González et al. (2009) for HPMC film-forming emulsions containing tea tree essential oil, homogenized under the same conditions. The kind of fatty acid greatly affected particle size distribution and $D_{3,2}$ and $D_{3,4}$ values ($p < 0.05$). Both parameters and the wideness of the distribution curve decreased as the chain length of saturated

Table 1
Particle size and viscosity of the film-forming emulsions (mean values and standard deviation).

Film	$D_{3,2}$ (μm)	$D_{4,3}$ (μm)	Viscosity (Pa s)
HPMC			0.0678 (0.0004)[a]
HPMC-LA	53 (2)[a]	84 (3)[a]	0.079 (0.005)[b]
HPMC-MA	4.7 (0.1)[b]	14.9 (0.2)[b]	0.081 (0.002)[b]
HPMC-PA	3.7 (0.1)[b]	13.0 (0.6)[b]	0.0789 (0.0001)[b]
HPMC-SA	1.91 (0.04)[c]	6 (1)[c]	0.0684 (0.0002)[a]
HPMC-OA	1.25 (0.01)[c]	1.43 (0.1)[d]	0.0685 (0.0003)[a]

[a–d]Different superscripts within a column indicate significant differences among formulations ($p < 0.05$). Data reported are mean values (standard desviation).

fatty acids increased. The presence of unsaturation in the case of oleic acid also promoted a decrease in these parameters. Lauric acid produced the biggest particles and poly-dispersion index, reflected in the greater difference between $D_{3,2}$ and $D_{3,4}$ values, whereas oleic acid gave rise to the smallest particles which were also the most homogeneous in size. The best dispersion in the aqueous system of oleic acid was also observed in the film-forming dispersion of sodium caseinate films containing fatty acids (Fabra et al., 2009), although as concerns the relationship between the chain length and the size of lipid aggregates, saturated fatty acids did not follow the same tendency as that obtained in HPMC solutions. Taking into account that the hydrophobicity of FA increases when the chain length increases, larger lipid micellar aggregates (bilayer or hexagonal micelles) would be expected when the chain length increased (Larsson & Dejmek, 1990). The opposite result obtained could be related with the interactions between fatty acids and HPMC. This fact and the high viscosity of HPMC solutions, could affect the micellar growth kinetics by making molecular mobility difficult, more so the bigger the molecules. In this sense, LA micelles could grow more than SA aggregates.

The greater polarity of the OA, reflected in its low critical micellar concentration (Mukerjee & Mysels, 1971) is coherent with the smaller lipid aggregates. More difficulties are expected for micellar growth during film drying, when the FA chains are longer, due to the fast increase in the viscosity of the continuous phase when the effective concentration of HPMC rises in line with the solvent evaporation.

3.1.2. Rheological behaviour

Rheological behaviour of film-forming emulsions was Newtonian in the shear rate range considered and viscosity values, obtained for each case, are shown in Table 1. Newtonian behaviour was also observed in previous studies for HPMC film-forming emulsions containing surfactants and HPMC concentrations between 1.5 and 4.5% (Villalobos, Hernández-Muñoz, Albors, & Chiralt, 2009). When the HPMC concentration in dispersions increased to 5%, shear thinning behaviour was observed (Sánchez-González et al., 2009). Table 1 shows that, whereas a significant increase in sample viscosity (almost 20%) was observed when lipids with the biggest aggregates (LA, MA and PA) were incorporated to the HPMC solution, no significant change in viscosity was obtained for the best dispersed lipids (SA and OA) which have significantly smaller lipid aggregates and longer chain lengths. The fact that the viscosity of the HPMC solution did not increase when 15% of OA or SA was dispersed, points to the fact that a part of the HPMC molecules could be linked to the lipid aggregates and so, do not contribute to the viscosity of the continuous phase. This aspect could be related with greater interactions between these FA and HPMC molecules, which favours the association of the polymer chains to the lipid structures, such as has been observed for other hydrocolloids (Erickson, 1990; Mondragón et al., 2008).

3.2. Characterization of the films

3.2.1. Structural properties

The study of the film microstructure, by using SEM or AFM, allows us to know the arrangement of the different components in the dried film which will be affected by the development during drying. In this period, the solvent evaporation provoked changes in the component concentrations and viscosity of the liquid phase, which leads to changes in the lipid aggregates and creaming phenomenon, thus affecting the internal and surface structure of the film and so, its final barrier, mechanical and optical properties (Villalobos, Chanona, Hernández, Gutiérrez, & Chiralt, 2005).

Fig. 2 shows the SEM micrographs of the cross-sections of the films. In the control film a homogeneous aspect was observed, with a continuous phase in the polymer matrix. In the other micrographs, discontinuities of different shapes and sizes were observed due to the presence of fatty acids. In films containing LA, MA and PA, a multilayered structure can be observed; the layers being larger for LA, reducing in size when the fatty acid chain length increases. These layers correspond to the separated lipids which crystallize as successive layers where the hydrocarbon chains are parallely oriented, offering the polar carboxylic groups to those corresponding to the parallel-adjacent layer (Larsson & Dejmek, 1990). These multilayer crystals are a result of the water loss of the lamellar micelles that are formed above a determined concentration of the lipid in an aqueous phase. The presence of hydrocolloids in the polar lipid-aqueous systems can modify or even inhibit the formation of the micellar structures mainly due to the hydrophobic interactions between the polymer chain and lipids (Tanford, 1980).

It is remarkable that lipid layers in the films were bigger when the particle size in the film-forming emulsions increased, which suggests that similar reasons that inhibit the growth of the lipid micelles during the emulsion homogenization act during the drying process leading to the film. One of these reasons may be the greater viscosity of the HPMC solution that increases during the film drying, inhibiting the molecular mobility necessary to micelle growth. This effect will be more notable when the lipid molecular weight increases and so, PA shows the smallest lipid layers. For stearic and oleic acids, a non-layered structure was observed and the lipids seem finely distributed in the polymer matrix, especially for OA. These two lipids also showed very small particles in the film-forming emulsion which, in turn, exhibited lower viscosity than the HPMC solution. These facts seem to indicate that particular polymer–lipid interactions occur that inhibit the lipid micellar growth both in the initial film-forming emulsions and during their drying.

Similar structures were found in previous studies for sodium caseinate films containing fatty acids, although in this case SA did form multilayer crystals in the film that greatly affected mass transfer properties (Fabra et al., 2009). Nevertheless, the same rela-

Table 2
Mean values (and standard deviation) of roughness parameters obtained from atomic force microscopy images R_a, R_q, and r (three images were analyzed in each case).

Film	R_a (nm)	R_q (nm)	r (%)[A]
HPMC	18 (9)a	28 (9)a	0.05 (0.02)a
HPMC-LA	564 (73)b	707 (47)b	7 (7)b,c
HPMC-MA	342 (39)c	433 (54)c	7 (6)c
HPMC-PA	304 (39)c	408 (86)c	2.6 (0.6)a,b,c
HPMC-SA	215 (27)d	270 (33)d	6.4 (0.3)b,c
HPMC-OA	94 (1)e	121 (1)e	0.9 (0.2)a,b

[a–e]Different superscripts within a column indicate significant differences among formulations ($p < 0.05$).

[A] The high variability of r for films containing LA and MA can be explained by the great size of particles (lipid layers) emerging in the film surface, close to the order of the surface area analyzed each time in AFM.

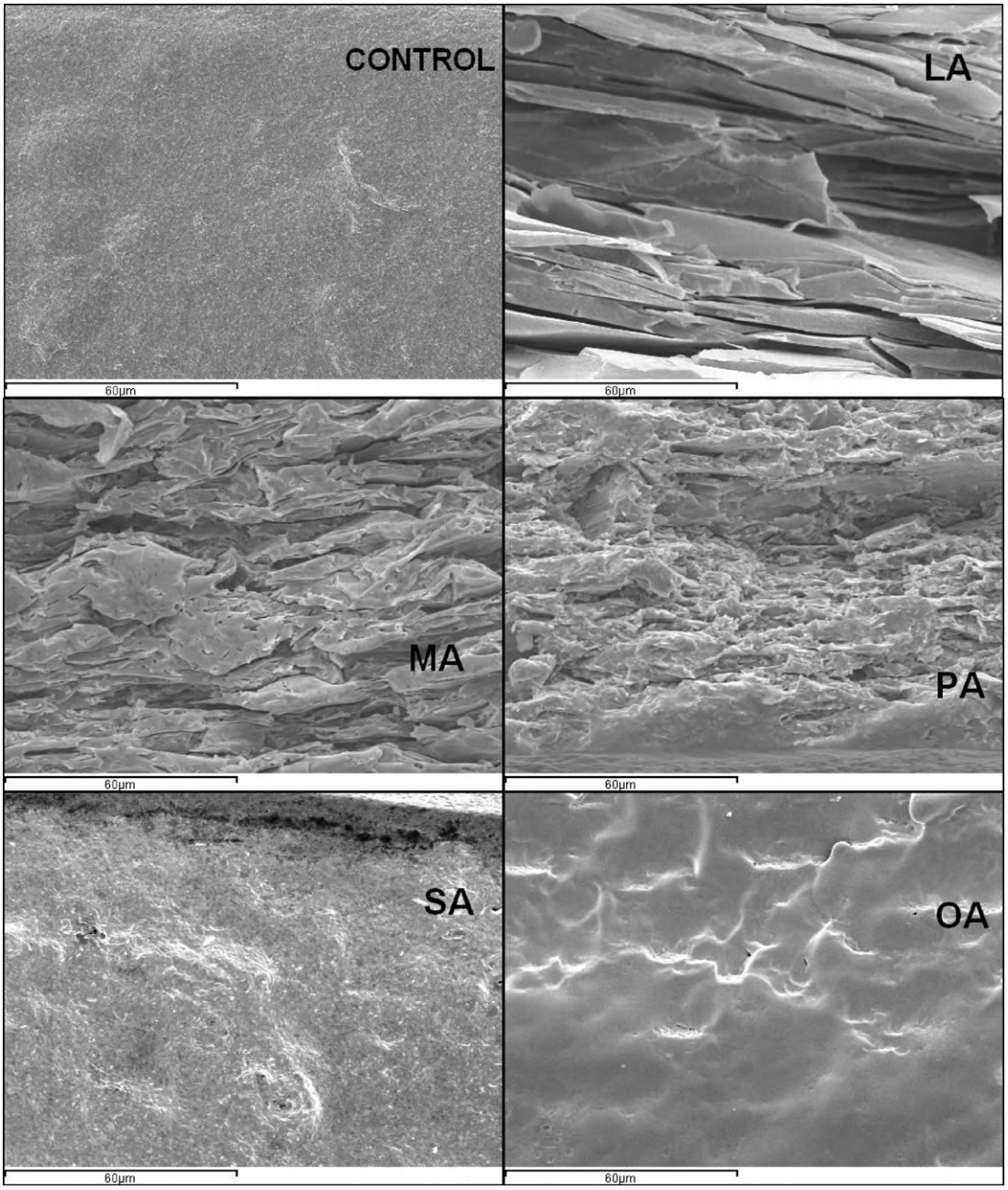

Fig. 2. SEM observations of cross-sections of the studied films.

tionship between the layer sizes and the molecular weight of the fatty acids was observed. The separation of lipid layers produced non-isotropic films in which the film top surface was enriched in lipid and the lower one was enriched in polymer, as has also been reported by other authors (Mc Hugh & Krochta, 1994).

The surface structure of the films was analyzed through AFM. This technique has been used previously in isolate edible films (Fabra et al., 2009; Mathew & Abraham, 2008; Villalobos et al., 2005) and in coated food products (Hershko & Nussinovitch, 1998). Fig. 3 shows the 3D-plots obtained for the height of the film with respect to a reference plane. The control film presents a smooth surface with very slight irregularities which can appear because of the presence of small dust particles. Incorporating fatty acids led to rougher film surfaces, as previously reported by Fabra et al. (2009) in sodium caseinate based films. The sizes of surface irregularities varied according to the different fatty acids and were coherent with the size of particles observed in the cross-section SEM images. LA shows the biggest surface reliefs whereas SA and OA show very small, but numerous, irregular formations. Table 2 shows the values of the roughness parameters (R_a, R_q, r), which described the 3D images obtained by AFM. R_a and R_q parameters showed a similar

Table 3
Mean values and standard deviation (in parentheses) of elastic modulus (EM), tensile strength (TS), and relative deformation (E) at break of films equilibrated at 58% relative humidity.

Film	EM × 10^{-1} (MPa)	TS (MPa)	E (%)
HPMC	255 (5)^{a}	55 (5)^{a}	7 (2)^{a}
HPMC-LA	138 (2)^{b}	17 (2)^{b}	1.5 (0.2)^{b}
HPMC-MA	179 (6)^{cd}	27 (2)^{c}	2.0 (0.3)^{bc}
HPMC-PA	193 (12)^{d}	33 (3)^{d}	3 (1)^{bc}
HPMC-SA	187 (20)^{d}	34 (3)^{d}	4 (1)^{c}
HPMC-OA	168 (8)^{c}	46 (7)^{e}	14 (3)^{d}

$^{a–d}$Different superscripts within a column indicate significant differences among formulations ($p < 0.05$).

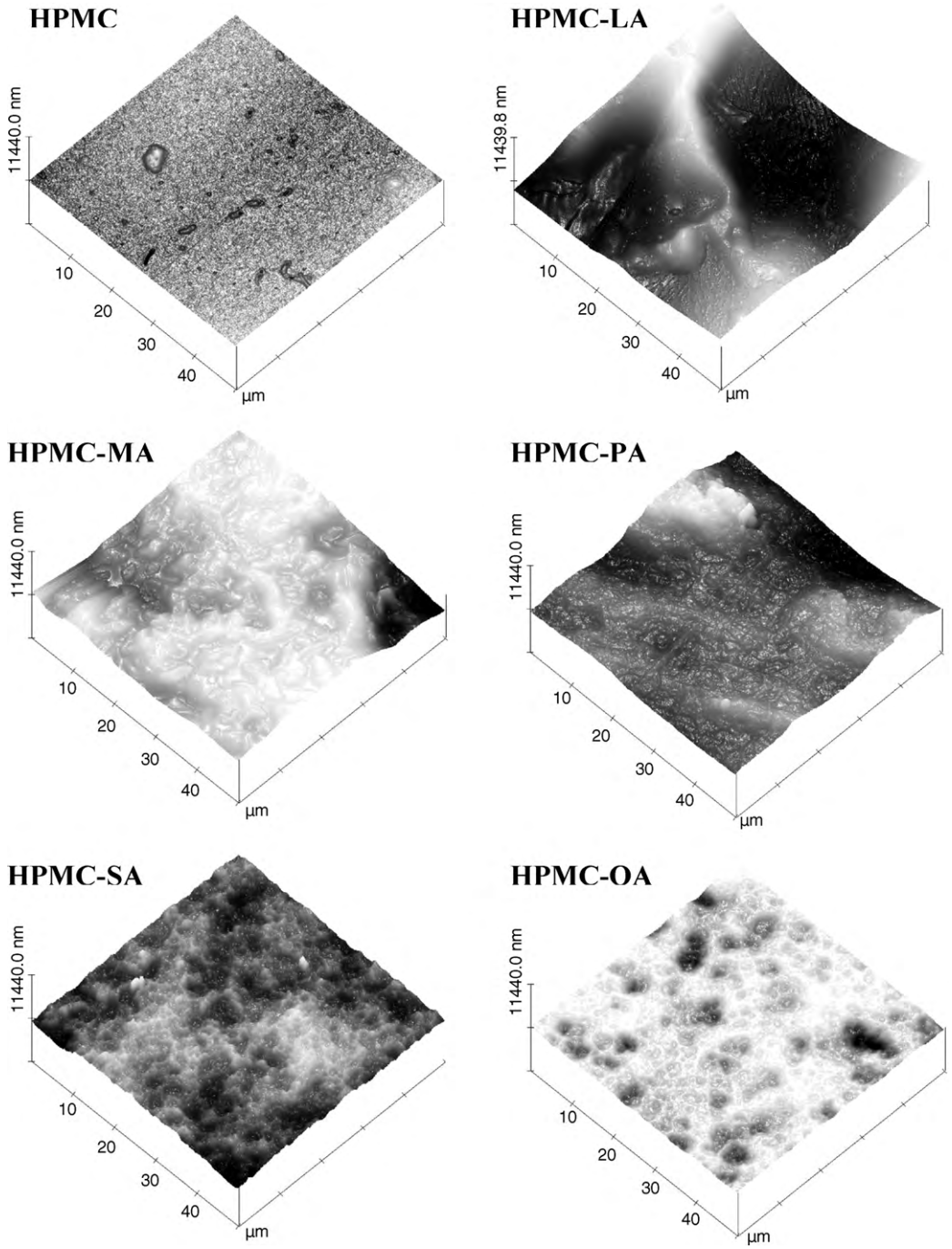

Fig. 3. 3D-plots obtained from AFM of control and lipid containing films.

behaviour for the films; the films containing LA showing the highest values due to the greatest height of the surface irregularities. On the contrary, OA gave rise to the lowest height of the surface reliefs. Small particles emerging on the film surface led to the lowest R_a and R_q values but could provoke relatively high r values when there are many particles present. This is the case of films containing SA. It is remarkable that, in terms of r values, very small differences could be observed for OA-containing films with respect to the control film, although the R_a and R_q values reflect the presence of surface particles of a significant height with respect to the reference plane.

3.2.2. Tensile properties

Analyzing the mechanical properties of an edible film is relevant in order to predict its behaviour when it has been applied to a food product. Elasticity modulus (EM), tensile strength (TS) and elongation at break (E) are very useful parameters for describing the mechanical properties of a film, and are closely related with its internal structure (Mc Hugh & Krochta, 1994).

Table 3 shows the results of the mechanical parameters obtained for each type of film. EM and TS values can be considered high if they are compared with those obtained by other authors for proteins (Fabra et al., 2009; Pérez-Gago & Krochta, 2001; Tanaka, Ishizaki, Suzuki, & Takai, 2001) and in the order of those obtained for HPMC films in similar conditions (Sánchez-González et al., 2009). The addition of fatty acids caused a significant decrease ($p < 0.05$) in elastic and resistance to break modulus due to the introduction of discontinuities in the polymer matrix of the dried film, at the same time as the deformation at break decreased (except in the case of

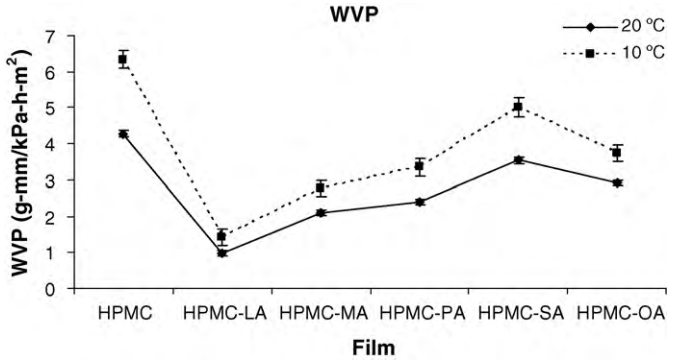

Fig. 4. Water vapour permeability of the films exposed to a relative humidity gradient of 54/58–100%, at two different temperatures (10 and 20 °C).

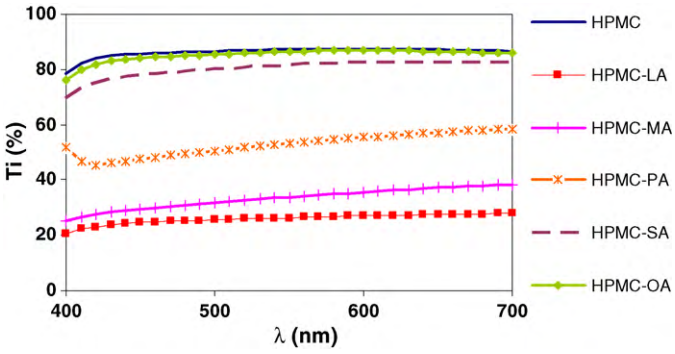

Fig. 5. Spectral distribution of internal transmittance (T_i) of control and lipid containing films.

OA). A similar effect was observed when other lipid components (essential oil) were added to HPMC based films (Sánchez-González et al., 2009). Nevertheless, differences in the load parameters could be observed for the different fatty acids which can be related with the developed film microstructure. In films which showed laminar structure, EM and TS decreased when the size of the lipid layers increased, which can be attributed to the greater mechanical resistance of the small particles than the big, taking into account the solid state of lipids under the conditions of the mechanical test.

The films containing SA or OA, which did not show lipid layers, behaved differently. Whereas SA showed parameters which were very close to those of the films containing PA, with very small laminar particles, OA produced a smaller decrease of the film's mechanical resistance with respect to the control and a remarkable increase of the film's stretchability. This behaviour can be explained by the liquid state of the OA, which allows the deformation of the lipid aggregate without break during the tensile test, and by the extremely fine dispersion of the lipid in the polymer matrix, probably promoted by a more marked affinity with the polymer and the development of interactions leading to a plasticizing effect, such as has been observed for other hydrocolloids like caseinates (Fabra et al., 2010). Similar results for the stretchability of films containing OA have been found by other authors working with different protein films (Monedero et al., 2009; Tanaka et al., 2001).

3.2.3. Water vapour permeability

Fig. 4 shows the WVP values obtained for HPMC films with and without fatty acids, at 10 and 20 °C. An almost parallel behaviour was observed for all the films as regards the effect of the temperature, showing a decrease of WVP as the temperature increases. Despite the expected increase in the molecular mobility in line with the increase in temperature, an opposite effect on this parameter was produced by the moisture content. In this sense, a greater water adsorption will occur in the hydrophilic matrix when temperature decreases and so, this can imply an overall increase of the water vapour diffusion through the hydrophilic network. This has also been observed in other works (Bertuzzi, Castro Vidaurre, Armada, & Gottifredi, 2007; Sánchez-González et al., 2009) and can be explained by the nature of adsorption–diffusion phenomena in films during moisture transport which the temperature affects in opposite ways. Whereas diffusion is favoured at high temperatures, molecular adsorption is promoted by low temperatures due to its exothermic nature. The greater difference of WVP between 10 and 20 °C corresponded to the control film, which proves that water adsorption in the HPMC matrix plays a predominant effect in moisture transfer across the films because of the greater water adsorption of the hydrocolloid than the fatty acid fraction. Regardless of temperature, the control film constituted the worst moisture barrier transfer. As expected, the addition of fatty acids reduced the WVP because of the increase of the film's hydrophobicity. This improvement of the water barrier properties has been found in previous works when lipid materials were added to the HPMC matrix (Hagenmaier & Shaw, 1990; Sánchez-González et al., 2009) and when fatty acids were added to protein based films (Fabra et al., 2009; Tanaka et al., 2001). Some authors report that WVP decreases as the chain length of lipids increases because the hydrophobicity in these films controls the water vapour transfer (Mc Hugh & Krochta, 1994; Tanaka et al., 2001). Nevertheless, the obtained results do not coincide with this and point to other effects related with the structural arrangement of the lipids in the film playing a more relevant role.

Fig. 4 shows that lipids which gave rise to the biggest laminar structures showed the best water vapour barrier properties, whereas a decrease in the barrier effectiveness were observed when the layers got smaller or when they disappeared (SA). The size of these layers is related with the size of the lipid aggregates in the film-forming emulsions and, in fact, a negative potential correlation between WVP and the mean particle size of micelles in the emulsion was observed ($r^2 = 0.980$ and 0.947 for $D_{4,3}$ and $D_{3,2}$ respectively), without considering films containing OA, which was not in the same tendency curve. OA films showed a lower permeability than that corresponding with the value of mean particle sizes which indicated that other factors affect WVP. The existence of specific interactions between oleic acid and HPMC chains, deduced from the analysis of the mechanical behaviour, could increase the matrix hydrophobicity. Similar results have been found for OA in caseinate films (Fabra et al., 2009).

3.2.4. Optical properties

According to Hutchings (1999), the most outstanding optical properties with which to evaluate the impact on the appearance and colour of coated products are opacity and gloss. High values of T_i are related with greater film homogeneity which corresponds with more transparent films. On the contrary, if lower values of T_i are obtained, the films are more opaque. Spectral distribution curves of T_i parameters are plotted in Fig. 5. These curves show that both the control film and the film with added oleic acid present similar spectrums, which indicates that the addition of oleic acid did not notably increase the HPMC film opacity. Nevertheless, when saturated fatty acids were added, the opacity increased as the size of the lipid aggregates increased in the matrix. The formation of layer structures during film drying produced a very anisotropic structure where refractive index changes occurred at each interface, which provoked highly intense light dispersion, giving rise to more opaque matrices. The decrease in the lipid layer size increases the opportunity for light transmission which promotes film transparency. The size of the lipid aggregates in the films (Fig. 2) and the obtained values of T_i wholly support this fact.

Table 4
Mean values (and standard deviation) of whiteness index and gloss values at 20°, 60° and 85° of the films.

Film	WI	Gloss 20°	Gloss 60°	Gloss 85°
HPMC	93 (1)[a]	70 (4)[a]	87 (6)[a]	93 (8)[a]
HPMC-LA	93.8 (0.3)[a]	3.1 (0.1)[b]	16 (2)[b]	12 (2)[b]
HPMC-MA	94.9 (0.2)[a]	1.3 (0.1)[b]	5.9 (0.2)[c]	16 (2)[b]
HPMC-PA	93 (2)[a]	0.8 (0.1)[b]	4.6 (0.2)[c]	20 (3)[b]
HPMC-SA	85 (1)[b]	0.4 (0.2)[b]	4.4 (0.7)[c]	18 (4)[b]
HPMC-OA	86 (1)[b]	1.3 (0.5)[b]	12.6 (1.3)[b]	33 (8)[c]

[a–c]Different superscripts within a column indicate significant differences among formulations ($p < 0.05$).

Table 4 shows the whiteness index (WI) values, obtained from the infinite reflection spectra, of HPMC and HPMC-fatty acid composite films. The observed values indicate that only oleic and stearic acid produced significant differences ($p < 0.05$) with respect to HPMC pure matrix. Nevertheless this causes no problem when the films are applied on a particular product due to the fact that they are highly transparent. On the contrary, the application of the other films (excluding the control) could cause problems due to their high opacity.

The obtained gloss values of the films measured at incidence angle values of 20°, 60° and 85° are shown in Table 4. The gloss values of the control film were the highest. This means that the pure matrix formed a smooth, rough-free surface, as has been seen in the AFM analysis. On the contrary, when fatty acids were added the gloss values greatly decreased. Lipid aggregation and creaming phenomena during film drying promote the presence of lipid particles on the film–air interface, causing a heterogeneous, much rougher surface. The relationship between the increase in the surface roughness and the gloss decrease in the films has been observed in different works (Fabra et al., 2009; Sánchez-González et al., 2009; Villalobos et al., 2005). For films that showed laminar structures (LA, MA and PA-containing films), a different tendency was observed for gloss values at 20° and 60° with respect to the values obtained at 85°; whereas at 85°, the gloss decreased when the lipid particle grew in size, the opposite behaviour was observed at 20° and 60°. In this sense, it is remarkable that for products with low gloss values (lower than 60 units at 60°), the measurements at the greatest angle are more representative, since gloss is promoted at this angle and a greater sensibility with which to observe differences among samples is achieved (Hutchings, 1999). So, values at 85° will be more adequate to evaluate the gloss of samples containing fatty acids. When these values were related with the roughness parameters, significant potential relationships were obtained ($G85° = 476R_a^{-0.58}$, $r^2 = 0.981$; $G85° = 665R_q^{-0.61}$, $r^2 = 0.972$; $G85° = 31r^{-0.37}$, $r^2 = 0.973$) in agreement with the marked reduction of gloss when the surface roughness increases, which in turn are intensely affected by the size of the lipid aggregates in the film.

4. Conclusion

The properties of HPMC edible films were greatly affected by the incorporation of fatty acids and a close correlation was observed between the microstructure developed in the films and physical properties. This microstructure was, in turn, greatly affected by the size/shape of the lipid aggregates in the initial film-forming emulsion and their development during film drying. Saturated FA with relatively short chain lengths formed bigger lipid micellar structures in the HPMC aqueous system than SA and OA, which grew notably during film drying, giving rise to crystallized lipid layers in the films. However, SA and OA did not form this laminar structure, showing finely distributed lipid aggregates in the polymer matrix. Differences in the molecular mobility, affected by the FA molecular weight and viscosity of the system or specific interactions of SA and OA with HPMC chains, may be responsible for the different behaviour. Laminar structures improved the moisture barrier properties, but resulted in more brittle and less stretchable films at the same time as the opacity increased and gloss was reduced. OA led to the films with the best properties, without increasing the opacity and reduced the WVP of HPMC to about 50%.

Acknowledgements

The authors acknowledge the financial support from the Spanish Ministerio de Ciencia e Innovación through Project AGL2007-65503/ALI, from the Conselleria de Educación de la Comunidad Valenciana through Project GVPRE/2008/355, and from the Vice-rectorate for Research of the UPV through Project PAID-06-08-3242. Alberto Jiménez Marco also thanks Conselleria de Educación de la Comunidad Valenciana for a FPI grant. Authors also thank Manuel Planelles and Jose Luis Mova from the UPV Electronic Microscopy Service for their assistance in the use of the SEM and AFM.

References

Albert, S., & Mittal, G. S. (2002). Comparative evaluation of edible coatings to reduce fat uptake in a deep-fried cereal product. *Food Research International*, *35*, 445–458.
ASME B46.1. (1995). *Surface texture: Surface roughness, waviness and lay, an American national standard*. New York: ASME.
ASTM. (1995). Standard test methods for water vapor transmission of materials. Standards Designations: E96-95. In *Annual book of ASTM standards*. Philadelphia, PA: American Society for Testing and Materials., pp. 406–413.
ASTM. (1999). *Standard test method for specular gloss. Designation (D523). Annual book of ASTM standards* Philadelphia, PA: American Society for Testing and Materials.
ASTM. (2001). Standard test method for tensile properties of thin plastic sheeting. Standard D882. In *Annual book of American standard testing methods*. Philadelphia, PA: American Society for Testing and Materials., pp. 162–170.
Baldwin, E. A., Nisperos-Carriedo, M. O., & Baker, R. A. (1995a). Edible coatings for lightly processed fruits and vegetables. *HortScience*, *30*, 35–38.
Baldwin, E. A., Nisperos-Carriedo, M. O., & Baker, R. A. (1995b). Use of edible coatings to preserve quality of lightly (and slightly) processed products. *Critical Reviews in Food Science and Nutrition*, *35*(6), 509–524.
Bertuzzi, M. A., Castro Vidaurre, E. F., Armada, M., & Gottifredi, J. C. (2007). Water vapor permeability of edible starch based films. *Journal of Food Engineering*, *80*, 972–978.
Bravin, B., Peressini, D., & Sensidoni, A. (2004). Influence of emulsifier type and content on functional properties of polysaccharide lipid-based edible films. *Journal of Agricultural and Food Chemistry*, *52*, 6448–6455.
Erickson, E. (1990). Lipid–protein interactions. In K. Larson, & S. E. Friberg (Eds.), *Food emulsions*. New York/Basel: Marcel Dekker, Inc.
Fabra, M. J., Jiménez, A., Atarés, L., Talens, P., & Chiralt, A. (2009). Effect of fatty acids and beeswax addition on properties of sodium caseinate dispersions and films. *Biomacromolecules*, *10*, 1500–1507.
Fabra, M. J., Talens, P., & Chiralt, A. (2010). Water sorption isotherms and phase transitions of sodium caseinate-lipid films as affected by lipid interactions. *Food Hydrocolloids*, *24*, 384–391.
Fernández, L., Díaz de Apodaca, E., Cebrián, M., Villarán, M. C., & Maté, J. I. (2007). Effect of the unsaturation degree and concentration of fatty acids on the properties of WPI-based edible films. *European Food Research and Technology*, *224*(4), 415–420.
Gómez-Estaca, J., Giménez, B., Montero, P., & Gómez-Guillén, M. C. (2009). Incorporation of antioxidant borage extract into edible films based on sole skin gelatin or a commercial fish gelatin. *Journal of Food Engineering*, *92*, 78–85.
Guilbert, S., Gontard, N., & Gorris, L. G. M. (1996). Prolongation of the shelf-life of perishable food products using biodegradable films and coatings. *Lebensmittel-Wissenschaft und-Technologie*, *29*(1, 2), 10–17.
Hagenmaier, R. D., & Shaw, P. E. (1990). Moisture permeability of edible films made with fatty acid and (hydroxypropyl) methylcellulose. *Journal of Agricultural and Food Chemistry*, *38*(9), 1799–1803.
Hershko, V., & Nussinovitch, A. (1998). Physical properties of alginate-coated onion (Allium cepa) skin. *Food Hydrocolloids*, *12*, 195–202.
Hutchings, J. B. (1999). *Food and colour appearance* (2nd edition). Gaithersburg, MD: Chapman and Hall Food Science Book, Aspen Publication.
Koelsch, C. M., & Labuza, T. P. (1992). Functional, physical and morphological properties of methyl cellulose and fatty acid-based edible films. *Lebensmittel-Wissenschaft und-Technologie*, *25*, 404–411.
Krog, N. J. (1990). Food emulsifiers and their chemical and physical properties. In K. Larsson, & S. E. Friberg (Eds.), *Food emulsions*. New York/Basel: Maecer Dekker, Inc.

Larsson, K., & Dejmek, P. (1990). Crystal and liquid crystal structures of lipids. In K. Larsson, & S. E. Friberg (Eds.), *Food emulsions*. New York/Basel: Maecer Dekker, Inc.

Mathew, S., & Abraham, E. (2008). Characterisation of ferulic acid incorporated starch-chitosan blend films. *Food Hydrocolloids*, *22*, 826–835.

Mc Hugh, T. H., Avena-Bustillos, R., & Krochta, J. M. (1993). Hydrophobic edible films: Modified procedure for water vapor permeability and explanation of thickness effects. *Journal of Food Science*, *58*(4), 899–903.

Mc Hugh, T. H., & Krochta, J. M. (1994). Water vapour permeability properties of edible whey protein–lipid emulsion films. *Journal of the American Oil Chemists Society*, *71*, 307–312.

Mecitoğlu, G. Ç., Yemenicioğlu, A., & Arslanoğlu, A. (2007). Antimicrobial and antioxidant activity of edible zein films incorporated with lysozyme, albumin proteins and disodium EDTA. *Food Research International*, *40*, 80–91.

Mondragón, M., Arroyo, K., & Romero-García, J. (2008). Biocomposites of thermoplastic starch with surfactant. *Carbohydrate Polymers*, *74*, 201–208.

Monedero, F. M., Fabra, M. J., Talens, P., & Chiralt, A. (2009). Effect of oleic acid-beeswax mixtures on mechanical, optical and barrier properties of soy protein isolate based films. *Journal of Food Engineering*, *91*(4), 509–515.

Mukerjee, P., & Mysels, K. J. (1971). *National standards reference data service* Washington, DC: National Bureau of Standards.

Pérez-Gago, M. B., & Krochta, J. M. (2001). Lipid particle size effect on water vapor permeability and mechanical properties of whey protein/beeswax emulsion films. *Journal of Agricultural and Food Chemistry*, *49*, 996–1002.

Sánchez-González, L., Vargas, M., González-Martínez, C., Chiralt, A., & Cháfer, M. (2009). Characterization of edible films based on hydroxypropylmethylcellulose and tea tree essential oil. *Food Hydrocolloids*, *23*(8), 2102–2109.

Tanaka, M., Ishizaki, S., Suzuki, T., & Takai, R. (2001). Water vapour permeability of edible films prepared from fish water soluble proteins as affected by lipid type. *Journal of Tokyo University of Fisheries*, *87*, 31–37.

Tanford, C. (1980). *The hydrophobic effect: Formation of micelles and biological membranes*. New York: Wiley.

Turhan, K. N., & Şahbaz, F. (2004). Water vapor permeability, tensile properties and solubility of methylcellulose-based edible films. *Journal of Food Engineering*, *61*(3), 459–466.

Villalobos, R, Chanona, J., Hernández, P., Gutiérrez, G., & Chiralt, A. (2005). Gloss and transparency of hydroxypropyl methylcellulose films containing surfactants as affected by their microstructure. *Food Hydrocolloids*, *19*, 53–61.

Villalobos, R., Hernández-Muñoz, P., Albors, A., & Chiralt, A. (2009). Barrier and optical properties of edible hydroxypropyl methylcellulose coatings containing surfactants applied to fresh cut carrot slices. *Food Hydrocolloids*, *23*, 526– 535.

Villalobos, R., Hernández-Muñoz, P., & Chiralt, A. (2006). Effect of surfactants on water sorption and barrier properties of hydroxypropyl methylcellulose films. *Food Hydrocolloids*, *20*, 502–509.